Shahid Chamran University of Ahvaz

Iranian Association of Electrical and Electronics Engineers

Journal of Applied Research in Electrical Engineering

E-ISSN: 2783-2864
P-ISSN: 2717-414X
Homepage: https://jaree.scu.ac.ir/

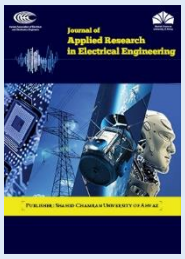

Research Article

Robustness Analysis of Model Reference Adaptive Controller in The Presence of Input Saturation Using Describing Function Method

Fatemeh Tavakkoli [1], Alireza Khosravi [1,*], Pouria Sarhadi [1,2]

[1] *Faculty of Electrical and Computer Engineering, Babol Noshirvani University of Technology, Babol 47148-71167, Iran*

[2] *Research Fellow in Autonomous Vehicles, Department of Mechanical Engineering Science, University of Surrey, Guildford, GU2 7XH, UK*

[*] *Corresponding Author: akhosravi@nit.ac.ir*

Abstract: This work represents a new method for robustness analysis of the model reference adaptive controller (MRAC) in the presence of input saturation. Saturation is one of the nonlinear factors affecting the stability of control systems which must be considered in controller design and stability analysis experiments. Various methods are presented for the stability and robustness analysis of adaptive control systems, and employment of describing function (DF) can be attractive and practical, due to the appropriate effectiveness of DF in estimating limit cycles and also the application of quasi-linearization theory. In this work, the stability analysis and a limit cycle estimation of a saturated system in the frequency domain are performed. The controller parameters are adjusted in a way that the system achieves its stable limit cycle in the presence of the initial conditions for the states. Moreover, the efficiency of the proposed method for second-order systems is reported in the presence of symmetric saturation and uncertainty model in Rohrs's counterexample as the unmodeled dynamics. The results demonstrate the proposed method provides a proper analysis of system stability during the changes in the control parameters and the saturation amplitude.

Keywords: Input saturation, unmodeled dynamic, describing function, frequency response, model reference adaptive control.

Article history
Received 22 June 2022; Revised 30 October 2022; Accepted 06 December 2022; Published online 29 March 2023.

How to cite this article
F. Tavakkoli, A. Khosravi, and P. Sarhadi, "Robustness analysis of model reference adaptive controller in the presence of input saturation using describing function method," *J. Appl. Res. Electr. Eng.*, vol. 2, no. 1, pp. 62-69, 2023.
DOI: 10.22055/jaree.2022.41169.1062

Check for updates

1. INTRODUCTION

The signal level that a stimulus can deliver is usually limited by physical or safety constraints. These limits exist in all control systems including force, torque, voltage, and flow. The impact of amplitude saturation in the design of control system often depends on the control system performance. This effect is ignored in some systems and an appropriate functioning of most systems occurs when the amplitude saturation is taken into account [1-2]. Therefore, the controller design in the presence of saturation and its identification has recently been studied. One of the first works to address this issue is metaheuristic-based optimization algorithms [3]. The saturated system is identified using different optimization methods and described the differences between them. in addition, due to the destructive effects of saturation on the system, many controllers are vulnerable to the nonlinear factors due to the performance changes of the closed-loop system that often cause an instability in the system. In order to solve this issue, anti-windup compensators are designed by investigating the effects and properties of saturation on the system and controller to guarantee stability of the system as well as preventing the occurrence of saturation in the control systems. These designs are based on different definitions of saturation effects [4]. The investigation of the stability analysis and the stabilization of linear systems is performed in the presence of saturation and different kinds of Lyapunov functions such as polyhedral, quadratic and Lure which are used to model the saturation section to analyze the behavior of the closed-loop nonlinear system [5]. Additionally, there are several methods for designing anti-windups such as LMI [6-8]. Accordingly, a coefficient can be determined based on the optimal solution of LMI, which affects the controller state equations and provides stability of the loop system [9]. Moreover, the compensation design is also proposed that the main idea is

that they combine Nussbaum gain technique into backstepping control to compensate the saturation input, mainly used in spacecraft [10]. Other types of compensators including nonlinear multi-input and multi-output (MIMO) systems [11], ship steering control [12], switched nonlinear systems [13], and hydro-turbine governing systems [14] are also introduced.

The model reference adaptive controller (MRAC) is an attractive method to design adaptive systems due to its acceptable performance. Accordingly, some compensators have been proposed for the MRAC in the presence of saturation. Modern compensators are used for the PID MRAC controller which is implemented on the practical system of the autonomous underwater vehicle (AUV) [15]. In addition to MRAC method, the positive μ method is proposed to reduce the saturation effects in the adaptive system in [16]. In the positive μ method, a coefficient known as μ is considered in the design of the control signal and affects the control signal when the system is saturated, consequently reduces the value of the signal. In addition to designing compensators in the presence of saturation, robustness analysis in the presence of unmodeled dynamics and uncertainties in a system is an important subject in the adaptive control [17]. Berk Altin and Kira Barton have shown how unmodeled dynamic (Rohrs counterexample [18]) causes instability in model reference adaptive iterative learning control (MRAILC) [19]. Eugene Lavretsky et al. have proposed a method based on the MRAC to investigate the general stability of the system with unmodeled dynamics [20]. The model reference adaptive controller was also used for the robustness of linear time-variant systems with temporal delay [21]. In these works, the stability analysis of the adaptive control system has been carried out with the Lyapunov function -albeit in the absence of saturation - and presented methods for the robustness of the controller.

One way to analyze the stability of nonlinear systems is the describing function. A frequency response method is a powerful tool for analyzing and designing linear control systems. However, frequency analysis cannot be applied directly for nonlinear systems because the frequency response function cannot describe the nonlinear system. Therefore, the describing function is used to approximate the analysis and estimate the nonlinear behaviors. The most important application of the describing function method is to estimate the limit cycle of nonlinear systems [22-24]. Additionally, the describing function has been examined in the analysis of nonlinear systems with memory [25-26]. Recently, the describing function is used for the robustness analysis of reference model adaptive systems in the presence of unmodeled dynamics and the describing function of the reference model adaptive controller [27].

In this work, the robustness of adaptive control systems to unmodeled dynamics has been upgraded to be used for second-order system with input saturation [27]. Adaptation, plant and saturation rules are converted into a lure model, which consists of a linear plant, nonlinear saturation on the forward path and an isolated nonlinear part in the feedback path. The describing function is then used to analyze the system in the frequency domain. By placing the DF of nonlinear parts and analysis via the Nyquist diagram, the prediction of the limit cycles of the system is achieved. The main goal of this work is to estimate the limit cycle the system and determine the approximate initial conditions for the adaptive system with nonlinear factors, which leads to the robustness of the system to reach its stable limit cycle. The application of the proposed method is investigated by simulating the second-order system in the presence of symmetric saturation and Rohrs counterexample as unmodeled dynamics. In addition, the rest of the paper is organized in a way to address the issues presented as follows. In Section II, the main problem is explained in the presence of saturation and the transformed parameters of the controller and the update rules obtained by transformations. In Section III, the describing function of the nonlinear parts is calculated and the limit cycle of the closed-loop system is estimated by drawing the Nyquist diagram. In Section IV, the second-order system with unmodeled dynamics and input saturation is included to indicate the usefulness of the proposed analysis method.

2. PROBLEM DESCRIPTION

In this section, the control system is explained in the presence of amplitude saturation. To simplify the analysis, new parameters are introduced, based on which updating rules are obtained. The second-order system under investigation has the following state equations (1).

$$\begin{cases} \dot{x}_p = A_p x_p + B_p(v(t) + f(x_p)) \\ f(x_p) = k_p x_p \end{cases} \quad (1)$$

where x_p is a state variable, $B_p \in R^{2\times1}$ and $A_p \in R^{2\times2}$ are known and constant, (A_p, B_p) are controllable, $f(x_p)$ is the linear state-dependent uncertainty, and $v(t)$ is the scalar input. The unmodeled dynamic is as (2):

$$\begin{cases} x_\eta = A_\eta x_\eta(t) + B_\eta U_{sat}(t) \\ v(t) = {C_\eta}^T x_\eta(t) \end{cases} \quad (2)$$

where $x_\eta \in R^{m\times1}$, $C_\eta^T \in R^{1\times m}$, and $A_\eta \in R^{m\times m}$ is a Hurwitz matrix with $G_\eta = C_\eta^T(sI_{m\times m} - A_\eta)^{-1}B_\eta$ and $(C_\eta^T, A_\eta, B_\eta)$ are controllable and observable, U_{sat} is the saturated control input which is defined as written in (3).

$$U_{sat}(u) = \begin{cases} u_{max} & if\ u > u_{max} \\ u \quad if\ -u_{max} < u < u_{max} \\ -u_{max} & if\ u < -u_{max} \end{cases}$$

$$u = \theta^T(t)x_p(t) \quad (3)$$

where u is the control input which is calculated by the controller, u_{max} is the maximum control signal that can be created by the stimulus, and $\theta^T(t) = [\theta_0\ \theta_1]$ are the adaptation rules (4) (refer to Fig. 1).

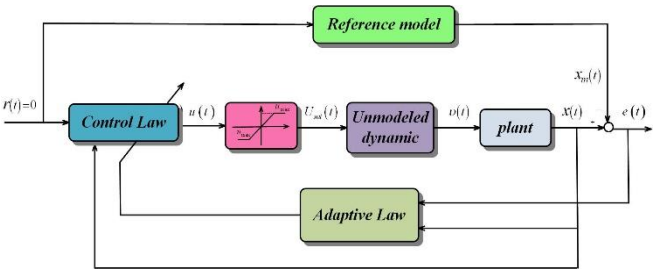

Fig. 1: The block diagram of the system in the presence of saturation.

$$\dot{\theta} = -\Gamma x_p {B_p}^T P\, e \tag{4}$$

where P is obtained from solving the Lyapunov.

In equations $A_m^T P + P A_m = -Q$, and $e = x_p - x_m$, x_m is the reference state variable and is defined as (5), and (6):

$$\dot{x}_m = A_m x_m + B_m r(t)$$
$$A_m = A_p + B_p \theta^{*T} \tag{5}$$
$$A_m = A_p + B_p(-{K_{LQR}}^T)$$
$$\theta^* = -{K_{LQR}}^T \tag{6}$$

where $r(t)$ is the reference input, A_m and B_m are the reference model state matrices, A_m is a Hurwitz matrix, and $\theta^{*T}(t) = [\theta_0^* \; \theta_1^*]$ are the ideal adaptive rules. A linear designing technique is employed to determine θ^{*T}. The linear-quadratic regulator (LQR) method is chosen as a tool for reference model control design. R_{LQR} and Q_{LQR} are its weight matrices and K_{LQR} is its vector for control parameters.

To simplify the analysis and determine the effect of saturation and unmodeled dynamic on the adaptive system, non-singular transformations are defined as equation (7):

$$\varepsilon(t) = Ce(t)$$
$$v(t) = M\theta(t) \tag{7}$$

where $\varepsilon(t)$ is the transformed error, $v(t)$ is the transformed parameter, C and M are the transform matrices. The transform matrices are defined as (8). The proof of the equations are expressed in reference [21-27].

$$C = [c_0 \quad c_1]^T \qquad M = p_b C P^{-1} \tag{8}$$

where $p_b = \sqrt{B_m^T P B_m}$, and C is defined as (9):

$$c_0 = {p_b}^{-1} P B_m \quad , \quad c_1 {c_1}^T = P - c_0 {c_0}^T \tag{9}$$

Remark 1 : From (8) and (9) the following equations can be obtained:

$${c^T}_0 B_m = p_b \quad , \quad {c^T}_1 B_m = 0$$
$$C P^{-1} C^T = I$$

Using (5) and (8) the $n \times n$ matrix below is determined as (10):

$$\tilde{A}_m = C A_m P^{-1} C^T = \begin{pmatrix} \alpha_{00} & a_1 \\ a_0 & \tilde{A}_m \end{pmatrix},$$
$$\alpha_{i,j} = {c_i}^T A_m P^{-1} c_j \qquad \forall i,j = \{0,1\} \tag{10}$$

where $\tilde{A}'_m \in R^{(n-1)\times(n-1)}$. It can be shown that $\tilde{A}'_m$ and $\tilde{A}_m$ are Hurwitz matrices. The error dynamic is defined as follows according to the closed loop system equation (11):

$$\dot{e} = A_m e + B_p \tilde{\theta}^T x_p + B_p \eta \tag{11}$$

where $\eta = v - U_{sat}$ is dependent on the saturated control input and the unmodeled dynamic, and $\tilde{\theta} = \theta - \theta^*$ is defined with θ^* in (6). The transformed error $\dot{\varepsilon}_i = C_i^T \dot{e}$ is obtained from (7) and (11) as equation (12).

$$\dot{\varepsilon} = \begin{bmatrix} {c^T}_0 A_m e + p_b \tilde{\theta}^T x_p + p_b \eta \\ {c^T}_1 A_m e \end{bmatrix} \tag{12}$$

Considering Remark1 and using (10) and (12) the equation (13) is concluded:

$$\dot{\varepsilon}_1 = \tilde{A}'_m \varepsilon_1 + a_0 \varepsilon_0 \tag{13}$$

$\dot{\varepsilon}_0$ can also be rewritten as (14):

$$\dot{\varepsilon}_0 = (\alpha_{00} + \tilde{v}_0)\varepsilon_0 + (a_1 + \tilde{v}_1)\varepsilon_1 + \ldots$$
$$\ldots + p_b \eta + \tilde{v}_0 m_0 + \tilde{v}_1 m_1 \tag{14}$$

where $v^* = M\theta^*$, $\tilde{v}_i = v_i - v_i^*$, and $m_i = C_i^T x_m$. The proposed adaptive rules are the revised standard adaptive rules using projection algorithm as (15).

$$\dot{\theta} = M^{-1}\dot{v}$$
$$\dot{v}_i = proj(\{M\theta\}_i, -\{M\Gamma x_p {B_m}^T P e\}_i) \tag{15}$$

where $\Gamma = \gamma P$

$$proj(\theta_i, y_i) = f(x) = \begin{cases} \dfrac{\theta_{i\,max}^2 - \theta_i^2}{\theta_{i\,max}^2 - \acute{\theta}_i^2}, & \theta_i \epsilon \Omega_i \Lambda \theta_i y_i > 0 \\ y_i, & Otherwise \end{cases}$$

$$\overline{\Omega_i} = \{\theta_i \epsilon \acute{R} | \theta'_{imax} \leq \theta_i \leq \theta_{imax}$$
$$\underline{\Omega_i} = \{\theta_i \epsilon \acute{R} | -\theta_{imax} \leq \theta_i \leq -\theta'_{imax}$$
$$\Omega_i = \overline{\Omega_i} \cup \underline{\Omega_i}$$

And the positive constant $\theta_{i,max} > \theta'_{i,max}$.

Remark 2 : It can be shown that if $\forall t \geq t_a \quad \|\theta_i(t_a)\| \leq \theta_{i,max} \Longrightarrow \|\theta_i(t)\| \leq \theta_{i,max}$ then the projection algorithm can guarantee the limitations of θ_i which is independent of the system dynamic.

Considering $\dot{v}_i = p_b C_i^T P^{-1} \theta$, and the transformed error as (16),

$$\dot{v}_i = \gamma' proj(v_i, (\varepsilon_i + m_i)\varepsilon_0) \tag{16}$$

in which $\gamma' = \gamma p_b^2$, Remark 2 guarantees that v_i^* will ultimately converge into the projection region.

3. DESCRIBING FUNCTION

The describing function is a classic tool to analyze the existence of the limit cycles in nonlinear systems based on the frequency response method [28]. The idea of the method is based on Gaussian linearization, so that the nonlinear part is considered as a single block, the describing function is a complex coefficient based on the main harmonics of the nonlinear system whose input is sinusoidal and its output is obtained through the Fourier series. The DF has many applications in nonlinear controllers and extensive researches have been performed where different methods such as Two-Sinusoid-Input Describing Function (TSIDF) and Dual-Input Describing Function (DIDF) have been proposed [26-29]. Despite the favourable characteristics of the describing functions, it is rarely used in adaptive control because of the complexity of the analysis of nonlinear systems with memory [29]. In a recent study, the stability of the MRAC is analyzed and the describing function of the controller is calculated using the DF method [25]. Although the DF is an approximate method, it is superior to other methods for nonlinear system analysis due to the desirable properties of the frequency response technique. In the following section, the method of the obtaining the function is introduced first, based on that,

the main system is divided into two linear and nonlinear parts. Then, the DF of the nonlinear sections is calculated and the stability analysis of the system will be provided via plotting the Nyquist diagram.

3.1. Calculating The Describing Function

If the nonlinear section is considered as a block with a sinusoidal input of amplitude A and the frequencyω, i.e., $x(t) = Asin(\omega t)$, its output, $w(t)$, is often a periodic function, despite it often being a non-sinusoidal (Fig. 1). Using the Fourier series, the periodic function $w(t)$ can be extended as (17):

$$w(t) = \frac{a_0}{2} + \sum_{n=1}^{\infty}[a_n\, cos(\,n\omega t) + b_n\, sin(\,n\omega t)] \tag{17}$$

where the Fourier coefficients a_n and b_n, which are often a function of A and ω, are determined by the equations below:

$$a_0 = \frac{1}{\pi}\int_{-\pi}^{\pi} w(t)d(\omega t)$$
$$a_n = \frac{1}{\pi}\int_{-\pi}^{\pi} w(t)\, cos(\,n\omega t)d(\omega t)$$
$$b_n = \frac{1}{\pi}\int_{-\pi}^{\pi} w(t)\, sin(\,n\omega t)d(\omega t)$$

The describing function should have some conditions, one of which being $a_0 = 0$. Furthermore, the main component is considered in the Fourier series. That is equation (18):

$$w(t) \approx w_1(t) = a_1\, cos(\,\omega t) + b_1\, sin(\,\omega t) = M\, sin(\,\omega t + \varphi) \tag{18}$$

where

$$M(A,\omega) = \sqrt{{a_1}^2 + {b_1}^2}$$
$$\varphi(A,\omega) = arctan(\frac{a_1}{b_1})$$

Equation (18) represents the main component corresponding to a sinusoidal input which is a sinusoidal with the same frequency as the input. This sinusoidal can be written as follows in a complex display as (19):

$$w_1 = Me^{j(\omega t+\varphi)} = (b_1 + ja_1)e^{j\omega t} \tag{19}$$

Similar to the concept of the frequency response function which was the ratio of the sinusoidal input and the sinusoidal output of a system in the frequency domain, the describing function of a nonlinear element is the complex ratio of the main component of the nonlinear element to the sinusoidal input. This means equation (20):

$$N(A,\omega) = \frac{Me^{j(\omega t+\varphi)}}{Ae^{j\omega t}} = \frac{M}{A}e^{j\varphi} = \frac{1}{A}(b_1 + ja_1) \tag{20}$$

3.2. Lure Model

The proposed controller is designed based on the proven concepts in [21-22] and it will be assumed for transforming into a lure model that $x_m(t_0) = 0$. Since it is assumed for analyzing the describing function that $r = 0$, therefore $\forall t \geq t_0\ \ x_m(t) = 0$ and $\forall t\ \ m_i(t) = 0$. Considering (14) and (16), the equation for the adaptive controller is as (21), and (22):

$$\dot{\varepsilon}_0 = (\alpha_{00} + \tilde{v}_0)\varepsilon_0 + (a_1 + \tilde{v}_1)\varepsilon_1 + p_b\eta$$

$$\dot{v}_i = -\gamma_i\varepsilon_0\varepsilon_i \tag{21}$$

where:

$$\gamma_i = \begin{cases} \dfrac{v_{imax}^2 - v_i^2}{v_{imax}^2 - v_{imax}'^2}, & if|v_i| \geq v_{imax}' \bigwedge -\varepsilon_0\varepsilon_i v_i > 0 \\ \gamma', & Otherwise \end{cases}$$

$$\gamma' = \gamma p_b^2$$

$$v_{i,max} = v_{i,max}' + \epsilon_i\ , \epsilon_i > 0 \tag{22}$$

Furthermore, from (21) we have $v_0 = -\gamma_1\varepsilon_0^2$. Thus v_0 is negative for all times if $v_0(t_0) > -v_{0,max}$. Hence, the parameter v_0 will ultimately converge to $v_{0,max}$ so, it is assumed that $v_0(t_0) = -v_{0,max}$. The control input is calculated according to Fig. 2 as follows:

$$u = {p_b}^{-1}v^T\varepsilon = {p_b}^{-1}(-v_{0,max}\varepsilon_0 + v_1\varepsilon_1) \tag{23}$$

where $v_{0,max}$ is a constant.

To separate the linear part from the nonlinear one, the plant and its unmodeled dynamic are considered as the linear block G_0, the section for updating the adaptation rules as a nonlinear block in the feedback, and the saturation is considered as a nonlinear block in the forward path (Fig. 3).

3.3. Analyzing the Describing Function (DF)

Typically, to compute the DF of the nonlinear part, all of it is considered as a single entity. Since there are two distinct nonlinear parts in here, the DF of each part is calculated individually. In order to obtain the DF of the adaptive rules section, it is assumed that one of its inputs is sinusoidal in the form of $\varepsilon_1 = A_1\sin(\omega_1 t)$ which is produced from the linear part according to Fig. 4. ε_0 is acquired by putting ε_1 in (13) where we will have equations (24) and (25).

$$\varepsilon_0(t) = \frac{A_1(\omega_1\, cos(\omega_1 t) - \tilde{A}_m'\ sin(\omega_1 t))}{a_0} \tag{24}$$

$$u(t) = \left(\frac{4\tilde{A}_m'A_1^3\varphi - 8a_0A_1v_{1,max}\omega_1 - 3A_1^3\gamma'\omega_1}{8a_0\omega_1p_b}\right)\sin(\omega_1 t) + \left(\frac{4A_1^3\omega_1 - 8A_1\tilde{A}_m'v_{0,max}\omega_1}{8a_0\omega_1p_b}\right)\sin(\omega_1 t) - \left(\frac{A_1^3\gamma'\tilde{A}_m' - 8A_1v_{0,max}\omega_1^2}{8a_0\omega_1p_b}\right)\cos(\omega_1 t)$$
$$\varphi = \tan^{-1}(\frac{\omega_1}{-\tilde{A}_m'}) \tag{25}$$

The obtained $u(t)$ is approximate. Hence, according to the definition of the DF in (20), with $\varepsilon_1 = A_1\sin(\omega_1 t)$ and the output in (25), the describing function of the nonlinear part in the feedback is acquired.

$$N_{A.L}(A_1,\omega_1) = \left(\frac{4\tilde{A}_m'A_1^2\varphi - 8a_0v_{1,max}\omega_1 - 3A_1^2\gamma'\omega_1}{8a_0\omega_1p_b}\right) + \left(\frac{4A_1^2\omega_1 - 8A_1\tilde{A}_m'v_{0,max}\omega_1}{8a_0\omega_1p_b}\right) - j(\frac{A_1^2\gamma'\tilde{A}_m' - 8v_{0,max}\omega_1^2}{8a_0\omega_1p_b}) \tag{26}$$

To obtain the describing function of the saturation

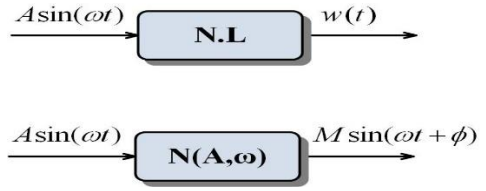

Fig. 2: The block diagram of a nonlinear element. Below: the display of its describing function [24].

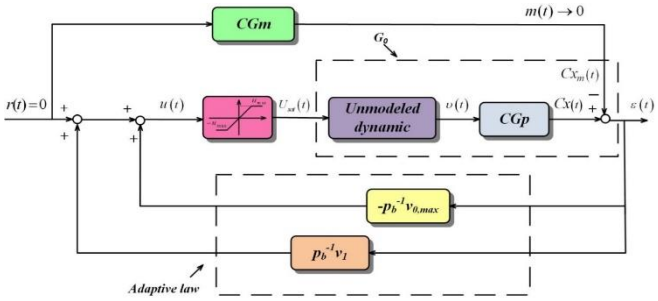

Fig. 3: The closed loop system with transformed states.

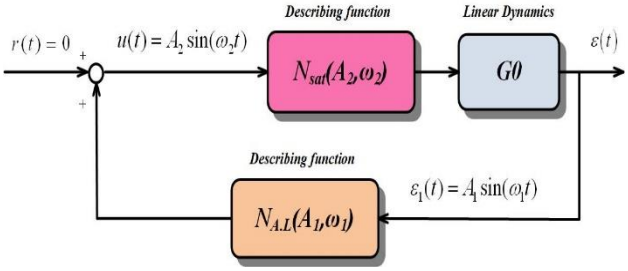

Fig. 4: The simplified block diagram of the closed loop system with the describing function.

section, it is assumed that $u(t) = A_2 \sin(\omega_2 t)$. This way if $A_2 > u_{max}$ then the describing function will be as equation (27):

$$N_{sat}(A_2) = \frac{2}{\pi}\left[\arcsin\left(\frac{u_{max}}{A_2}\right) + \frac{u_{max}}{A_2}\sqrt{1-\left(\frac{u_{max}}{A_2}^2\right)}\right] \quad (27)$$

and if $A_2 < u_{max}$ then $N_{sat}(A_2) = 1$. The performance of the DF is that it allows the stability analysis of a nonlinear system in the frequency domain to be evaluated in the same manner as linear systems. Consider the system in Fig. 4 where the describing function of nonlinear elements is placed instead of the elements themselves. If it is assumed that $\varepsilon_1 = A\sin(\omega t)$ then the frequency response of the close-loop will be:

$$G_0(j\omega)N_{A.L}(A,\omega)N_{sat}(A) + 1 = 0$$
$$\Rightarrow G_0(j\omega)N_{A.L}(A,\omega)N_{sat}(A) = -1 \quad (28)$$

Therefore, the describing function can be used to present the stability and robustness of the closed-loop nonlinear systems in a graphical form, such as the Nyquist diagram. In this way that the Nyquist diagram of the linear part of the system $G(j\omega)$ can be plotted as usual and the describing function $-1/(N_{A.L}(A,J\omega)N_{sat}(A))$ for different amplitudes on the same axes. In this way, the intersection point of the two diagrams shows the amplitude and the frequency of the limit cycle. Alternatively, the diagram of $G(j\omega)N_{A.L}(A,\omega)N_{sat}(A)$ is drawn for different amplitudes similar to the Nyquist diagram. Then, the point '-1' is the point where the oscillation can occur [30]. It can be assumed stability analysis that the sinusoidal input has some phase, that is $\varepsilon_1(t) = A\sin(\omega t + B)$. Accordingly, there are two equations and three variables for acquiring the limit cycle. Thus, the obtained solution will not be unique anymore. Therefore, it is assumed that the main harmonic does not have any phase.

Finally, given the initial conditions, it is observed that the obtained estimation for the limit cycle is correct and its amplitude and frequency has a very slight difference with the value acquired from the analysis. In the next section, this method is applied to a second-order system.

4. Simulation Example

In this section, the intended method for stability analysis is simulated for a practical plant. By introducing the system in (1), the describing function of the adaptive rules in (26), and saturation in (27), the amplitude and frequency of the limit cycle will be achieved using (28), and after the analysis with the Nyquist diagram, the system is given the initial conditions. The analysis will be repeated for different values of the controller parameter and the saturation amplitude. The system of generic transport aircraft (DC-8) airplane is considered as the main system in the proposed method [31].

$$\begin{pmatrix}\dot{\alpha}\\ \dot{q}\end{pmatrix} = \underbrace{\begin{pmatrix}\frac{Z_\alpha}{V} & 1+\frac{Z_q}{V}\\ M_\alpha & M_q\end{pmatrix}}_{A_p}\underbrace{\begin{pmatrix}\alpha\\ q\end{pmatrix}}_{x_p} + \underbrace{\begin{pmatrix}\frac{Z_\delta}{V}\\ M_\delta\end{pmatrix}}_{B_p}\Lambda\left(\upsilon(t) + f(x_p)\right)$$
$$f(x_p) = f(\alpha, q) = K_\alpha\alpha + K_q q$$

where α(deg) is the aircraft angle of attack, q(deg/s) is the pitch rate, V(ft/s) is the air speed (considered constant), $M_\delta, M_q, M_\alpha, Z_\delta, Z_q, Z_\alpha$ are the stability converters of the plane, $\Lambda > 0$ is the loss of control effectiveness, and $f(x_p)$ is the uncertainty of the dynamics of the system.

$$A_p = \begin{pmatrix}-0.8060 & 1.0\\ -9.1486 & -4.59\end{pmatrix} \quad B_p = \begin{pmatrix}-0.04\\ -4.59\end{pmatrix}$$
$$\Lambda = 0.5 \quad , \quad K_\alpha = 1.5M_\alpha \quad , \quad K_q = 0.5M_q \quad (29)$$

highly damped second-order unmodeled dynamics [18-27], described by

$$G_\eta = \frac{{\omega_n}^2}{s^2 + 2\zeta\omega_n s + {\omega_n}^2}$$
$$with \quad \zeta = 0.9912 \quad \omega_n = 15.1327 \quad (30)$$

The control signal δ_e (deg) is the elevator deflection in this system and control rules for determining the reference model are obtained using the LQR method with weight matrices of $R_{LQR} = 1$ and $Q_{LQR} = diag(0.5,0.5)$. Other unknown parameters are selected as (31):

$$\gamma' = 1, u_{max} = 30 \quad B_m = \begin{pmatrix}1\\ 0\end{pmatrix}, Q = \begin{pmatrix}0.2 & 0\\ 0 & 40\end{pmatrix} \quad (31)$$

It can be shown that:

$${\tilde{A}_m}' = 1.4995, \quad a0 = 31.22, \quad \theta^* = [-0.0178 \quad 0.2185]^T$$

$\upsilon_{0,max}$ and $\upsilon_{1,max}$ are selected to be 5 and 3.2 respectively. The value for the amplitude and the frequency of the limit cycle is obtained to be $A^* = 27$ and $\omega^* = 6.28$ using (28).

Moreover, if all parameters are adjusted then G0 and $N_{A.L}$ are showed according to (32). Since the frequency of the limit cycle is determined by the plant, three different values are observed for the amplitude by drawing the Nyquist diagram for $G_0(j\omega)N_{total}(j\omega)$. As the amplitude is reduced, the diagram will circle around the point '-1' and vice versa. As explained before, the amplitude whose Nyquist diagram crosses the '-1' point is the amplitude of the limit cycle. Fig. 5 depicts the Nyquist diagram of the system for three different values of amplitudes.

$$G0(S) = \frac{-4.58S - 546.6}{S^4 + 30.4S^3 + 282.9S^2 + 1346S + 9567}$$
$$N_{A.L}(A^* + j\omega^*) = -2.6432 - 1.7036i \quad (32)$$

Other amplitudes and frequencies may apply to (28) such as $A = 5.5$ and $\omega = 16.5$. But a limit cycle is stable if all of the paths around it will ultimately converge to it and these conditions are formulated as below:

$$\frac{\partial(\Im(-N(A,\omega)G_0(j\omega)))}{\partial\omega}|_{A^*,\omega^*} > 0$$
$$\frac{\partial(\Re(-N(A,\omega)G_0(j\omega)))}{\partial A}|_{A^*,\omega^*} > 0$$

Eventually, considering the system in (1), and (29), the unmodeled dynamic in (2), (30), the saturation in (3), the reference model in (5), and the adaptation rules in (31), the stable initial condition is acquired by changing the initial conditions $\varepsilon_1(0)$ and other initial conditions as follows:

$$x_m(0) = 0\ ,\ x_\eta(0) = 0$$
$$x_p(0) = C^{-1}\varepsilon(0)\ ,\ \varepsilon_0(0) = 0.35\varepsilon_1(0)$$

Also, the controller parameters are as below:

$$v_{0max} = 5, \epsilon_0 = 0.1v_{0max}, v_{1max} = 3.2, \epsilon_1 = 0.02v_{1max}$$
$$v_{imax} = v'_{imax+}\epsilon_i$$

In Fig. 6, the transformed error is displayed for two different initial values. Regarding the obtained values for the amplitude and frequency from the analysis, it is observed that the describing function method could successfully predict the limit cycle and according to the practical features of the system, the initial conditions of the states were less than 30 degrees.

The saturated control signal for this limit cycle is almost similar to the saturated control signal which is obtained by applying a sinusoidal input with the amplitude and frequency of the limit cycle. These two signals will approximately coincide with each other in most times because the limit cycle reaches its stability and this shows the appropriate initial conditions and the correct estimation of the limit cycle (Fig. 7).

As seen in (27), and (28), it is obvious that the DF is dependent on $v_{0,max}$, $v_{1,max}$ and u_{max}. This means that by changing these values, the limit cycle of the system will change. By changing the amplitude from 30 to 15 and the controller parameters being constant $v_{1,max} = 3.2$, and $v_{2,max} = 5$, the values $A = 45.5$ and $\omega = 6.3$ are obtained for the limit cycle from the frequency analysis. This limit cycle is shown in Fig. 8 for two different initial conditions.

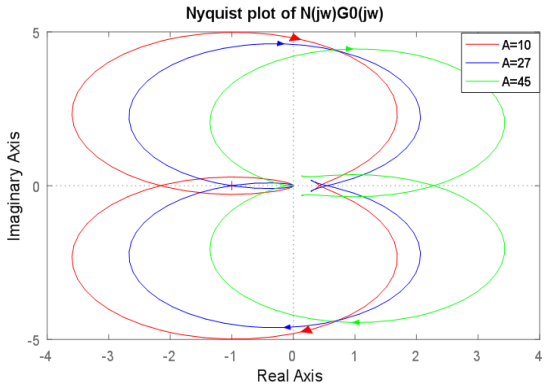

Fig. 5: The Nyquist diagram of $G(j\omega)N(A,\omega)$.

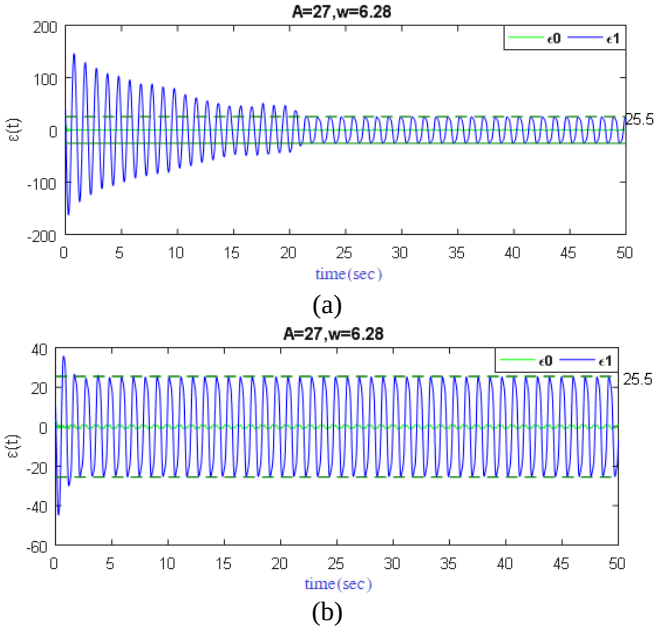

Fig. 6: The display of the stable limit cycle for two different initial conditions and the values $u_{max} = 30$, $v_{1,max} = 3.2$, and $v_{0,max} = 5$, (a) $\varepsilon_1(0) = 38$ and $x_p(0) = [15.6 \quad 20.9]^T$, and (b) $\varepsilon_1(0) = 10$ and $x_p(0) = [4.14 \quad 5.5]^T$.

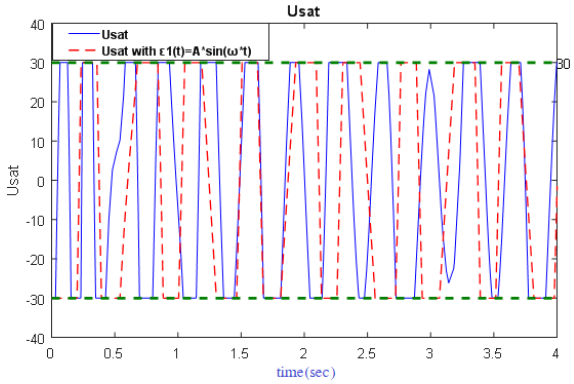

Fig. 7: The saturated control signal with $u_{max} = 30$ and the initial conditions of $\varepsilon_1(0) = 10$ and the next with the input $\varepsilon_1(t) = A^* sin(\omega^* t)$.

Now, if the values are set to $v_{0,max} = 0.2$, and $v_{1,max} = 1.3$ and the saturation amplitude stays constant $u_{max} = 15$, the

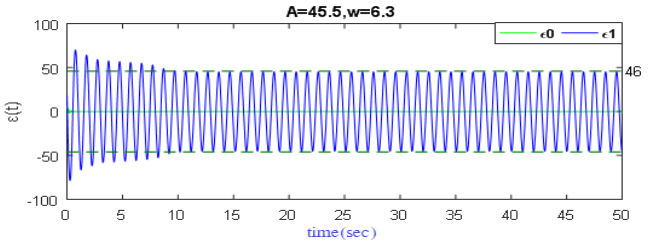

(a)

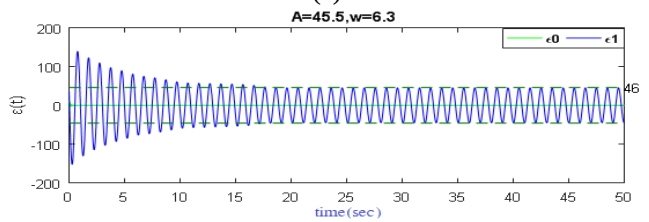

(b)

Fig. 8: The stable limit cycle for $u_{max} = 15$, $v_{0,max} = 0.2$ and $v_{1,max} = 1.3$, (a) The transformed error for initial conditions $\varepsilon_1(0) = 18$ and $x_p(0) = [7.4 \quad 9.8]^T$, and (b) The transformed error for initial conditions $\varepsilon_1(0) = 35$ and $x_p(0) = [14.5 \quad 19.3]^T$.

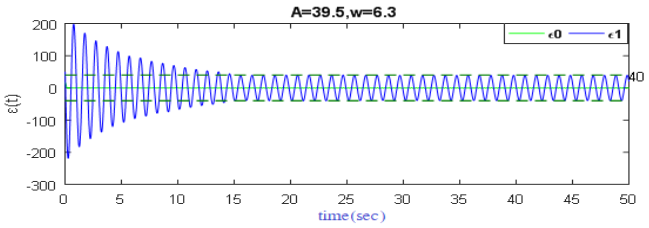

(a)

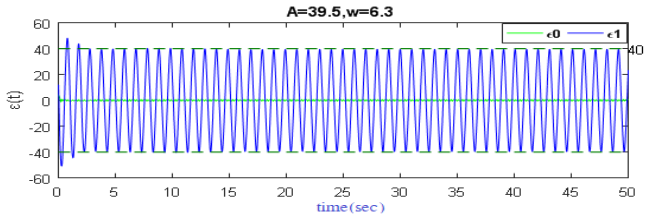

(b)

Fig. 9: The stable limit cycle for $u_{max} = 15$, $v_{0,max} = 0.2$, and $v_{1,max} = 1.3$, (a) The transformed error for initial conditions $\varepsilon_1(0) = 50$ and $x_p(0) = [20.7 \quad 27.46]^T$, and (b) The transformed error for initial conditions $\varepsilon_1(0) = 12$ and $x_p(0) = [4.96 \quad 6.6]^T$.

amplitude and the frequency of the limit cycle are acquired as $A = 39.5$ and $\omega = 6.3$ from the analysis. As seen in Fig. 9, the numerical simulation confirms the estimation obtained from the DF method. The limit cycle has a slight difference with the results of the analysis, the difference can be attributed to the describing function method because it is an approximate analytical method. The control signal and the saturated control signal for these updates and saturation parameters with the initial conditions $x_p(0) = [4.96 \quad 6.6]^T$ are shown in Fig. 10.

5. Conclusion

In this work, an accurate stability analysis method for the model reference adaptive controller for second-order systems

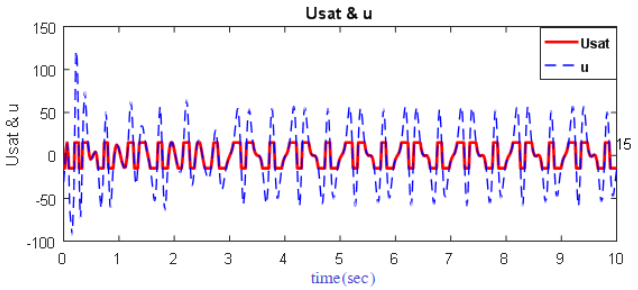

Fig. 10: The control signal and the saturated control signal for initial conditions $\varepsilon_1(0) = 12$, $u_{max} = 15$, $v_{0,max} = 0.2$, and $v_{1,max} = 1.3$.

in the presence of saturation, unmodeled dynamics and the uncertainty of the system has been proposed. The recognition of the effects of nonlinear factors such as saturation in the stability analysis of systems is undeniable. Since the describing function is one of the accurate methods for nonlinear systems analysis and in the general system, there were two nonlinear parts including saturation and the nonlinear adaptive controller, the DF method was employed for the stability analysis of the system and to predict the stable limit cycles. Using this analytical method, the accurate estimation of the limit cycle was performed and the parameters of the applied algorithm were adjusted in the MRAC and conditions were established so that the system reached its stable limit cycle given the initial conditions of variables. One of the main features of the proposed method is the use of frequency analysis to predict the limit cycles of the system and the correct approximation of their amplitude and frequency. The simulation results demonstrate the integrity of the method for second-order systems by changing the saturation amplitude and the controller adjustment parameter.

CRediT Authorship Contribution Statement

Fatemeh Tavakkoli: Formal analysis, Software, Writing - original draft, Writing - review & editing. **Alireza Khosravi:** Conceptualization, Supervision, Validation. **Pouria Sarhadi:** Validation, Supervision.

Declaration of Competing Interest

The authors declare that they have no known competing financial interests or personal relationships that could have appeared to influence the work reported in this paper. The ethical issues; including plagiarism, informed consent, misconduct, data fabrication and/or falsification, double publication and/or submission, redundancy has been completely observed by the authors

References

[1] D. S. Bernstein, and A.N. Michel, "A chronological bibliography on saturating actuators," *International Journal of robust nonlinear control*, vol. 5, no. 5, pp. 375-380, 1995.

[2] V. Kapila, and K. Grigoriadis, *Actuator Saturation Control*, ser. Control Eng. New York, NY: Marcel Dekker, 2002.

[3] Sarhadi, P., A. Khosravi, and V. Bijani, "Identification of nonlinear actuators with time delay and rate saturation

using meta-heuristic optimization algorithms," *Proceedings of the Institution of Mechanical Engineers, Part I: Journal of Systems Control Engineering*, vol. 229, no. 9, pp. 808-817, 2015.

[4] P. Hippe, *Windup in control: its effects and their prevention*. Springer Science & Business Media, 2006.

[5] S. Tarbouriech, et al., *Stability and stabilization of linear systems with saturating actuators*. Springer Science & Business Media, 2011.

[6] S. Galeani et al., "A magnitude and rate saturation model and its use in the solution of a static anti-windup problem," *Systems & Control Letters*, vol. 57, no. 1, pp. 1-9, 2008.

[7] K. Kefferpütz, B. Fischer, and J. Adamy, "A nonlinear controller for input amplitude and rate constrained linear systems," *IEEE Transactions on Automatic Control*, vol. 58, no. 10, pp. 2693-2697, 2013.

[8] N Wada, and M. Saeki, "Anti-windup synthesis for a model predictive control system," IEEJ Trans Elec Electron Eng., vol. 11, no. 6, pp. 776-785, 2016.

[9] D. Li, N. Hovakimyan, and C. Cao, "Positive invariant set estimation of adaptive controller in the presence of input saturation," *International Journal of Adaptive Control Signal Processing*, vol. 27, no. 11, pp. 1012-1030, 2013.

[10] Q. Hu, X. Shao, Y. Zhang, L. Guo, "Nussbaum-type function–based attitude control of spacecraft with actuator saturation," *Int J. Robust Nonlinear Control*, vol. 28, no. 8, pp. 2927-2949, 2018.

[11] A. Gelb, and W. E. Van der Velde, Multiple-input describing functions and non-linear system design. 1968.

[12] C. Y. Tzeng, and K. F. Lin, "Adaptive ship steering autopilot design with saturating and slew rate limiting actuator," *International Journal of Adaptive Control Signal Processing*, vol. 14, no. 4, pp. 411-426, 2000.

[13] J. Zhang, and T. Raïssi, "Saturation control of switched nonlinear systems," *Nonlinear Analysis: Hybrid Systems*, vol. 32, pp. 320-336, 2019.

[14] Z. Peng, and W. Guo, "Saturation characteristics for stability of hydro-turbine governing system with surge tank," *Renewable Energy*, vol. 131, pp. 318-332, 2019.

[15] P. Sarhadi, A. R. Noei, and A. Khosravi, "Model reference adaptive PID control with anti-windup compensator for an autonomous underwater vehicle." *Robotics and Autonomous Systems*, vol. 83, pp. 87-93, 2016.

[16] M. C. Turner, "Positive μ modification as an anti-windup mechanism," *Systems & Control Letters*, vol. 102, pp. 15-21, 2017.

[17] P. A. Ioannou, and J. Sun, *Robust adaptive control*. Courier Corporation, 2012.

[18] C. Rohrs, L. Valavani, M. Athans, G. Steinet, "Robustness of continuous-time adaptive control algorithms in the presence of unmodeled dynamics," *IEEE Transactions on Automatic Control*, vol. 30, no. 9, pp. 881-889, 1985.

[19] B. Altın, and K. Barton, "Rohrs' example revisited: On the robustness of adaptive iterative learning control," *Asian Journal of Control*, vol. 20, no. 3, pp. 993-1002, 2018.

[20] H. S. Hussain, M. Matsutani, A. M. Annaswamy, and E. Lavretsky, "Robust adaptive control in the presence of unmodeled dynamics: A counter to Rohrs's counterexample," in *AIAA Guidance, Navigation, and Control (GNC) Conference*, American Institute of Aeronautics and Astronautics, 2013.

[21] M. Matsutani, A. Annaswamy, and E. Lavretsky. Guaranteed delay margins for adaptive systems with state variables accessible," in *2013 American Control Conference*, IEEE, 2013.

[22] D. Atherton, and S. Spurgeon, *Nonlinear Control Systems, Analytical Methods*, Wiley Encyclopedia of Electrical and Electronics Engineering, 1999.

[23] K. S. Narendra, and A. M. Annaswamy, *Stable adaptive systems*, Courier Corporation, 2012.

[24] J. -J. E. Slotine, and W. Li, *Applied nonlinear control*. Vol. 199, Prentice Hall Englewood Cliffs, NJ, 1991.

[25] R. Sridhar, "A general method for deriving the describing functions for a certain class of nonlinearities," *IRE Transactions on Automatic Control*, vol. 5, no. 2, pp. 135-141, 1960.

[26] Vander Velde, W.E., Multiple-input describing functions and nonlinear system design. 1968: McGraw-Hill, New York.

[27] H. S. Hussain, C. S. Subedi, A. M. Annaswamy, and E. Lavretsky, "Robustness of adaptive control systems to unmodeled dynamics: A describing function viewpoint," in *AIAA Guidance, Navigation, and Control Conference*, American Institute of Aeronautics and Astronautics, 2017.

[28] L. T. Aguilar, I. Boiko, L. Fridman, and R. Iriarte, *Self-oscillations in dynamic systems*, Springer, 2015.

[29] J. E. Gibson, *Nonlinear automatic control*, McGraw-Hill Book Company, New York, 1963.

[30] C. Fielding, and P. Flux, "Non-linearities in flight control systems," *The Aeronautical Journal*, vol. 107, no. 1077, pp. 673-686, 2003.

[31] E. Lavretsky, and K. Wise, *Robust and Adaptive Control: With Aerospace Applications*. Springer, 2012.